Solid-Liquid Mass Transfer in Packed Beds with Cocurrent Downward Two-Phase Flow

Ana Lakota
Janez Levec
Department of Chemistry and Chemical Technology
University of Ljubljana
61000 Ljubljana, Yugoslavia

Various hydrodynamic regimes are formed in the trickle bed reactor depending on the structure of the packed bed, the particle wettability, the fluid physical properties and velocities. At moderate liquid and gas flow rates, both phases are continuous and result in the low interaction or trickling flow regime (LIR). In this regime, the gas does not affect the liquid texture, but the external surface of the particles may not be entirely wetted by the liquid phase. In the high interaction regime (HIR), the flow rates of the phases are usually higher, which can lead to one of several possible flow regimes. The pulsing and spray flow regimes were observed by Charpentier and Favier (1975), while Talmor (1977) additionally noted the dispersed-bubble and bubble-pulse flow regimes. As pointed out by many investigators, various key parameters such as pressure drop, liquid holdup, and heat and mass transfer rates all depend on the flow regime that exists in the packed bed.

A significant amount of research has been performed on the measurement of mass transfer properties between flowing liquid and solid particles. Generally, two experimental techniques have been employed: 1. the dissolution of slightly soluble packing into water (Goto et al., 1975; Hirose et al., 1976; Specchia et al., 1978; Satterfield et al., 1978); and 2. an electrochemical method (Chou et al., 1979; Rao and Drinkenburg, 1985). In both cases of the LIR and HIR, the mass transfer rate has been found to increase always with increasing liquid flow rate. In the LIR, however, there is some disagreement in the literature on the effect of gas flow rate on the liquid-solid mass transfer coefficient. For example, Hirose et al. (1976) found that the gas flow rate had no effect, while Satterfield et al. (1978) reported an increase of about 10% within the trickling flow regime. Evidence to date suggests that the transition from LIR to HIR should result in a step increase in mass transfer rate. Accordingly, Rao and Drinkenburg (1985) noted a threefold increase when entering the pulsing flow regime. Higher mass transfer rates could be ascribed, in addition to the obvious influence of the higher intrinsic liquid velocities, to the improved wetting efficiency (Chou et al., 1979) and to the effect of the gas phase on the liquid-solid mass transfer mechanism through the local turbulence (Rao and Drinkenburg, 1985).

One of the main goals of this study was to determine how the liquid-solid mass transfer rate is affected by the gas flow in a trickle-bed operated in both the low (LIR) and high (HIR) interaction regimes. The volumetric liquid-solid mass transfer coefficients were measured by means of the dissolution of naphthalene cylinders into water. Dynamic liquid holdup was measured simultaneously to evaluate the intrinsic velocity of a liquid. The liquid-solid mass transfer rates were also studied in liquid-full operation. Results from both modes were used to determine the fraction of external surface area of packing that was wetted in a three-phase system and, consequently, the liquid-solid mass transfer coefficient alone. Finally, a single correlation for the liquid-solid mass transfer coefficient, valid for both the LIR and HIR, is proposed.

Experimental System

The experimental system used in this study is described in a previous paper by Levec et al. (1986).

Naphthalene cylinders were prepared from a mixture of naphthalene powder that was well mixed with talc and stearate (10.8 and 1.2 wt. %, respectively). The 6.1 × 4.7 mm cylinders were pressed out with a side crush strength of 15 kg. The cylinders were randomly packed in each column segment to maintain the bed porosity independent of the bed length. For several hours prior to making the experimental measurements, they were exposed to high liquid and gas flow rates. After this pretreatment in which the surface texture of the cylinders underwent a change, reproducible measurements in mass transfer rates were achieved.

The solubility of naphthalene in water at 13°C was determined spectrophotometrically to be 29 mg/L at 274 nm. To keep the potential for the dissolution of naphthalene between 25% and 75%, the length of the packing had to be changed during the experiments. Properties of the bed and packing are listed in Table 1.

Table 1. Properties of Column and Packing

Column diameter, m	0.172
Packing length, m	0.32, 0.62 and 1.225
Dimension of cylinders (dia. × length)	
Before experiments, mm	6.1 × 4.7
After experiments, mm	5.9 × 4.5
Average equivalent diameter, mm	5.45
Porosity of cylinders (Hg porosimetry)	0.10
Bed porosity	0.31
Static holdup	0.037
Surface area per unit volume, m^{-1}	749
Column to particle diameter ratio	31

Dynamic liquid holdups were determined by using the gravimetric method as described in detail by Levec et al. (1986). The absorbance of the effluent water was measured simultaneously by a UV-detector (Milton-Roy) and reached a constant value after 10 to 20 minutes. In a typical run, the gas flow rate was kept constant and the liquid flow rate was gradually increased. Two runs were also made, each at fixed value of liquid flow rate, while the gas flow rate was increased. The range of operating conditions used in this work are summarized in Table 2.

The volumetric liquid-solid mass transfer coefficients were calculated from the following equation

$$k_s a = \frac{\Phi_l}{A \cdot z} \ln \frac{ABS^*}{ABS^* - ABS} \tag{1}$$

which assumes plug flow of the liquid phase. ABS^* and ABS are the absorbance of saturated water and of column effluent water, respectively.

In the present work, the following hydrodynamic regimes were identified by visual means and pressure drop measurements: trickle flow, pulse flow, bubble flow, and dispersed bubble flow. Since the column was made of plexiglass, the contours of air bubbles were easily observed on a light background of naphthalene cylinders wetted by water.

Results and Discussion

Figure 1 shows the measured dynamic liquid holdup vs. the liquid Reynolds number (Re_l). The liquid Reynolds number used here is based on the interstitial velocity of liquid and hydraulic radius. The various flow regimes observed in our experiments are also presented which include the trickling or low interaction regime, the bubble flow regime, and the dispersed bubble flow and pulse flow regimes. The latter three are collectively considered here to be the high interaction regime. For higher values of the gas mass velocity, the transition from

Table 2. Range of Operating Conditions

	Liquid Tap Water	Gas Air
Temperature, °C	13	13
Mass velocity, $kg/m^2 \cdot s$	0.72 – 43	0.003 – 0.294
Liquid Reynolds no., Re_l	4.7 – 282	
Mod. liquid Reynolds no., Re_l^*	15 – 600	

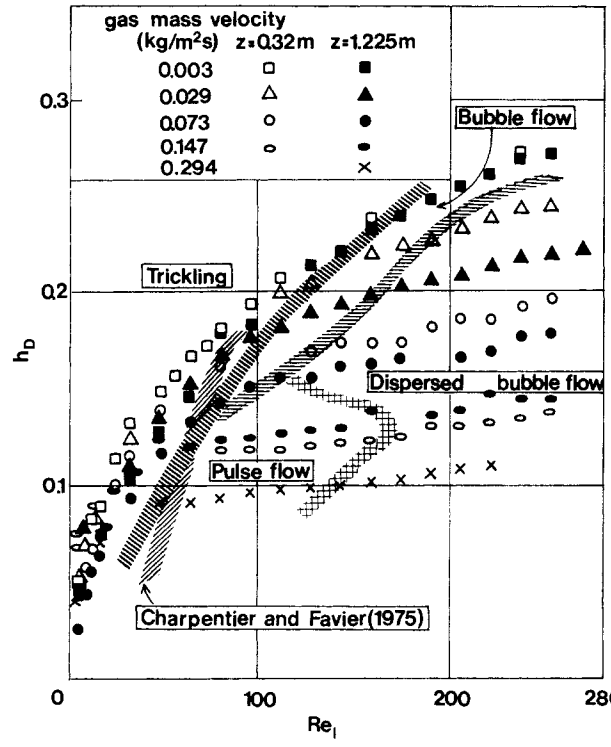

Figure 1. Dynamic liquid holdup as a function of liquid Reynolds number and flow regimes visually observed in two-phase flow.

LIR to HIR occurs at lower liquid mass velocity. Our transition line at various gas mass velocities is in close agreement with the one obtained by Charpentier and Favier (1975).

The effect of the gas mass velocity on liquid holdup is rather small at low Re_l. As the transition from the LIR to the HIR occurs, the gas mass velocity strongly influences the dynamic liquid holdup. Increased gas mass velocity decreases dynamic liquid holdup.

Figure 1 also shows that the dynamic liquid holdup is influenced by the bed height since longer beds have less holdup than shorter beds. The differences are certainly not within the experimental errors. The possibility that the flow regime was not fully developed in shorter beds is not supported by the experimental facts. In contrast, these facts imply that the liquid was more evenly distributed in shorter beds. The distributor was visually observed to provide an excellent liquid and gas-phase distribution at the top of the bed. Therefore, any channeling and maldistribution of liquid, both of which reduce the liquid holdup, occurred deeper in the bed. It should also be noted that the naphthalene cylinders, with diameter to length ratio greater than one, formed an unusual packing structure. This packing consisted of many "strings," in which cylinders touched one another by the flat surfaces. These strings probably had the greatest contribution on the liquid maldistribution and relatively low porosity of the bed.

The measured volumetric liquid-solid mass transfer coefficients vs. Re_l at different gas mass velocities are shown on Figure 2. The coefficients increase smoothly with liquid Reynolds number over the whole range of operating conditions. No sharp

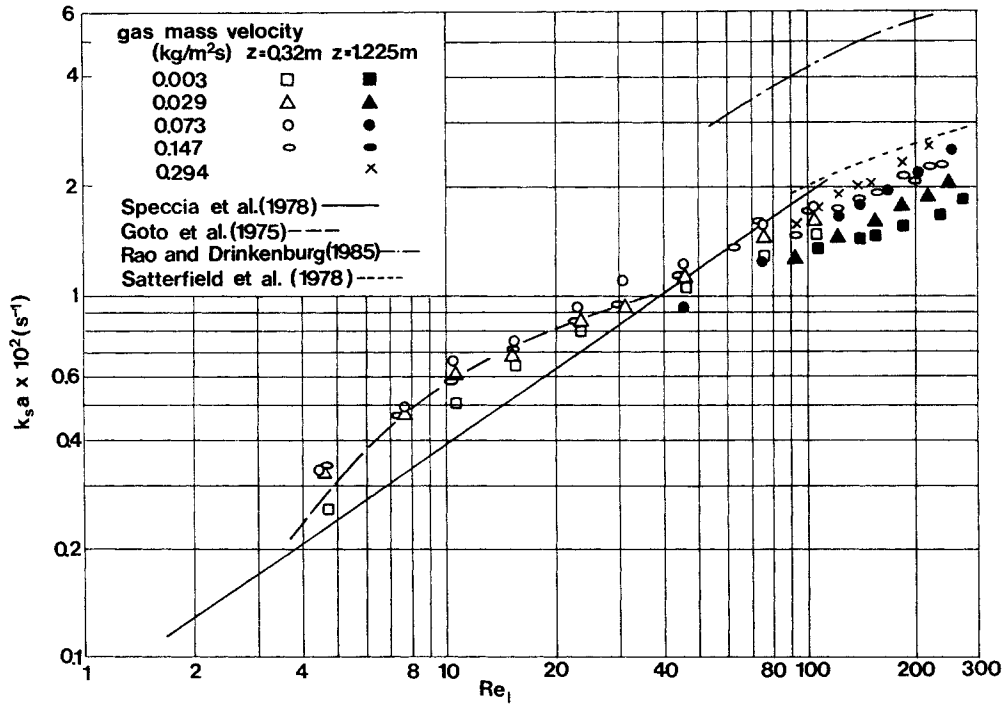

Figure 2. Volumetric liquid-solid mass transfer coefficients as a function of liquid Reynolds number for two-phase flow.

discontinuity in the $k_s a$ values were found when the hydrodynamic regime changed in the reactor (see Figure 1 for the transition lines). It is obvious that a simple power-law correlation of the volumetric mass transfer coefficients using this form of the Reynolds number is not justified and another approach is necessary.

Figure 2 shows that the gas mass velocity has a noticable effect on the mass transfer rate. An increase of gas mass velocity (from 0.003 kg/m^2 · s to 0.294 kg/m^2 · s) increases the volumetric liquid-solid mass transfer coefficients by 30% in the LIR and over 50% in the HIR. An increase in $k_s a$ with the gas mass velocity was also confirmed in the experiments, where the liquid flow rate was kept constant and the gas mass velocity was gradually increased. The results of these measurements were within 15% of those illustrated in Figure 2.

In the LIR, our data agree quite well with those measured by Goto et al. (1975), while the correlation of Specchia et al. (1978) slightly underestimates them. In the HIR, the predictions of Satterfield et al. (1978) also agree reasonably with our results while the correlation proposed by Rao and Drinkenburg (1985) overpredicts the data by about a factor of two. The last two correlations employ an energy dissipation function which requires the knowledge of pressure drops and liquid holdups. In these calculations, a gas mass velocity of 0.294 kg/m^2 · s and pressure drop data of Lakota (1990) were used.

In Figure 3, the measured liquid-solid mass transfer coefficients are replotted using a modified liquid Reynolds number Re_l^* which is based on the intrinsic velocity of the liquid over the particles. Using the dynamic liquid holdup data from Figure 1, the intrinsic velocity v_l^* was calculated using

$$v_l^* = \frac{\Phi_l}{A h_D} \tag{2}$$

The new liquid Reynolds number was then defined as

$$Re_l^* = \frac{Re_l \epsilon_B}{h_D} \tag{3}$$

where the dynamic liquid holdup h_D in Eq. 3 is equal to the bed porosity for liquid-full operation.

Figures 2 and 3 show that the data collapse into one line and smoothly increase with Re_l^*. The results have higher scatter at low Re_l^*, but this is probably due to the experimental errors involved in the dynamic liquid holdup measurements (Levec et al., 1986). The transition from LIR to HIR at different gas flow rates occurs at a Re_l^* of approximately 160 which is estimated from Figure 1. Figure 3 indicates that the gas velocity has no significant effect on the mechanism of liquid-solid mass transfer as long as the liquid Reynolds number is based on the intrinsic velocity of the liquid over the particles. The gas flow increases $k_s a$ in the trickle bed only through decreasing the dynamic liquid holdup. This, in turn, increases the intrinsic liquid velocity.

In Figure 3, the volumetric mass transfer coefficients from the liquid-full operation mode are shown also. At low Re_l^* (up to 70), these data are higher than the two-phase data indicating that the particles in the trickle-bed are not completely wetted. To account for the wetting efficiency, a comparison was made between the volumetric liquid-solid mass transfer coefficients in the two-phase flow to those in single-phase (liquid) flow at the same intrinsic velocity of the liquid

$$f_w = \left[\frac{(k_s a)_{\text{two-phase flow}}}{(k_s a)_{\text{single-phase flow}}}\right] \text{at the same } v_l^* \tag{4}$$

The results of applying Eq. 4 to the data are illustrated in Figure

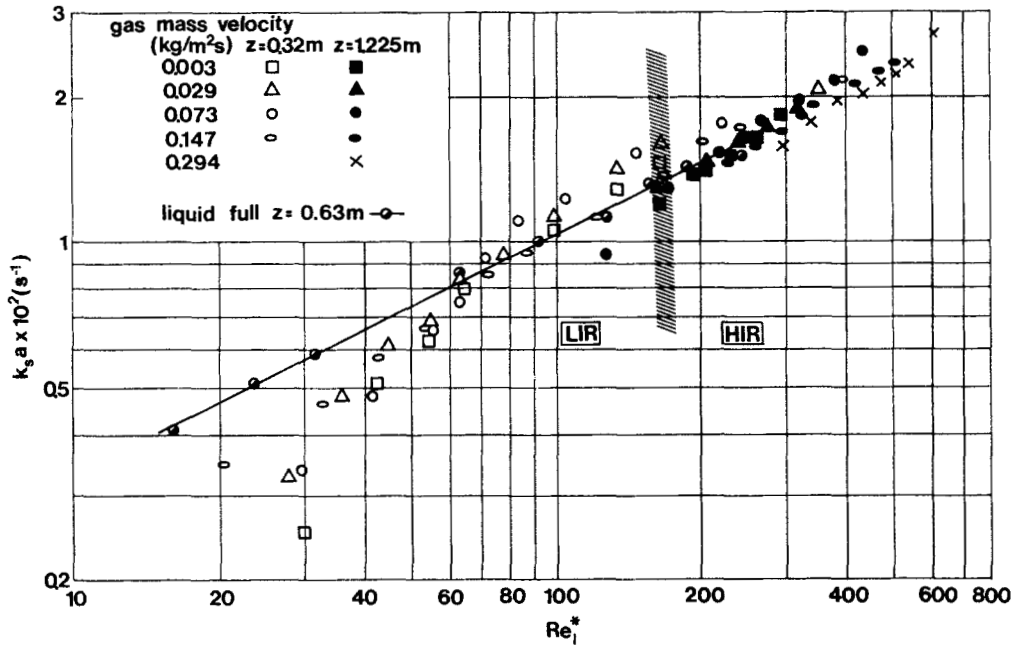

Figure 3. Volumetric liquid-solid mass transfer coefficients as a function of modified liquid Reynolds number for two-phase and single-phase (liquid) flow.

4. The wetting efficiency increases with increasing liquid mass velocity between 0.6 and 1 except at the lowest value of the gas mass velocity. Experimental errors in h_D measurements made the data at the lowest value of the gas mass velocity unreliable. Rather large scattering in f_w did not allow us to find the effect of gas flow on the wetting efficiency.

The experimental wetting efficiencies are within the range reported by Satterfield (1975) and also agree well with the data of other investigators. The correlation of Mills and Duduković (1981, 1982) seems to be very useful for the prediction of wetting efficiency.

The liquid-solid mass transfer coefficients k_s were extracted from the measured $k_s a$ using the wetting efficiency f_w and the following relation

$$k_s = \frac{k_s a}{f_w a_t} \tag{5}$$

where a_t is the geometrical surface area of the particles per unit

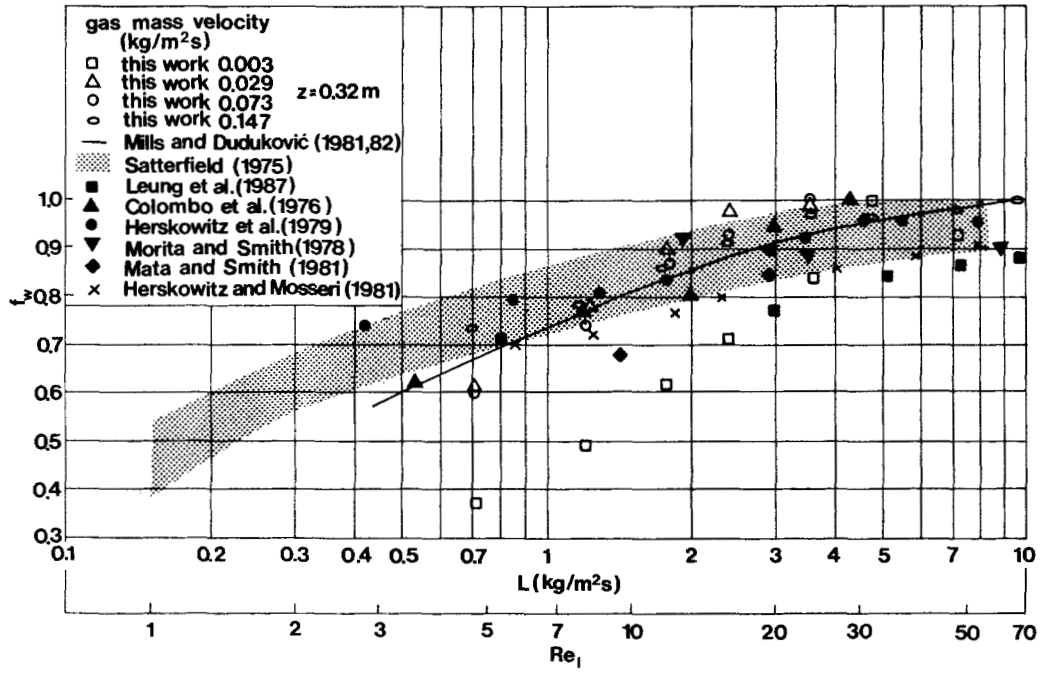

Figure 4. Wetting efficiency as a function of liquid Reynolds number for two-phase flow.

volume of the bed. The k_s values calculated from the two-phase data at low Re_l^* where the particles were not entirely wetted (Figure 3) fitted to those obtained in single-phase flow operation. So, for the whole range of operating conditions the k_s vs. Re_l^* data can be correlated using simple power-law form:

$$\frac{Sh}{Sc^{1/3}} = 0.487\ (Re_l^*)^{0.495} \tag{6}$$

provided $15 \leq Re_l^* \leq 600$ and $Sc = 2216$. The mean relative deviation (MRD) of 7.2% was found when compared to 81 points. It is worth noting that the 0.495 power on the modified Reynolds number is close to the 0.5 power that would be predicted by boundary-layer theory.

Acknowledgment

The authors acknowledge support from the US-Yugoslav Joint Fund for Scientific and Technological Cooperation, in cooperation with the National Science Foundation under Grant No. INT-8509375.

Notation

A = column cross section, m^2
a_t = total external area of particles per unit volume of bed, m^{-1}
D = diffusivity of solute in liquid, $m^2 \cdot s^{-1}$
d_e = average equivalent particle diameter defined as six times the volume to surface ratio, m
f_w = wetting deficiency
h_d = dynamic holdup per unit volume of bed
k_s = liquid-solid mass transfer coefficient, $m \cdot s^{-1}$
$k_s a$ = volumetric liquid-solid mass transfer coefficient, s^{-1}
Re_l = liquid Reynolds number, $(\phi_l/A\epsilon_B)(\rho/\mu)d_e(\epsilon_B/1-\epsilon_B)$
Re_l^* = modified liquid Reynolds number, $Re_l\epsilon_B/h_d$
Sh = Sherwood number, $(k_s/D)d_e(\epsilon_B/1-\epsilon_B)$
Sc = Schmidt number, $(\mu/\rho D)$
v_l^* = intrinsic liquid velocity, defined by Eq. 2, $m \cdot s^{-1}$
z = packing length, m

Greek letters

ϵ_B = bed porosity
μ = liquid viscosity, $kg \cdot m^{-1} \cdot s^{-1}$
ρ = liquid density, $kg \cdot m^{-3}$
Φ_l = liquid volumetric flow rate, $m^3 \cdot s^{-1}$

Literature Cited

Charpentier, J. C., and M. Favier, "Some Liquid Holdup Experimental Data in Trickle-Bed Reactors for Foaming and Nonfoaming Hydrocarbons," *AIChE J.*, **21,** 1213 (1975).

Chou, T. S., F. L. Worley, and D. Luss, "Local Particle-Liquid Mass Transfer Fluctuations in Mixed Phase Cocurrent Downflow Through a Fixed Bed in the Pulsing Regime," *Ind. Eng. Chem. Fund.*, **18,** 279 (1979).

Goto, S., J. Levec, and J. M. Smith, "Mass Transfer in Packed Beds with Two-Phase Flow," *Ind. Eng. Chem. Process Des. Dev.*, **14,** 473 (1975).

Herskowitz, M., R. G. Carbonell, and J. M. Smith, "Effectiveness Factors and Mass Transfer in Trickle-Bed Reactors," *AIChE J.*, **25,** 272 (1979).

Herskowitz, M., and S. Mosseri, "Global Rates of Reaction in Trickle-Bed Reactors: Effects of Gas and Liquid Flow Rates," *Ing. Eng. Chem. Fund.*, **22,** 4 (1983).

Hirose, T., Y. Mori, and Y. Sato, "Liquid-to-Particle Mass Transfer in Fixed Bed Reactor with Cocurrent Gas-Liquid Downflow," *J. Chem. Eng. Japan,* **9,** 220 (1976).

Lakota, A., "Hydrodynamics and Mass Transfer Characteristics of Trickle-Bed Reactor," PhD Thesis, Dept. of Chem. and Chem. Tech., Univ. of Ljubljana, Yugoslavia (1990).

Leung, P. C., F. Recasens, and J. M. Smith, "Hydrogenation of Isobutene in a Trickle-Bed Reactor: Wetting Efficiency and Mass Transfer," *AIChE J.*, **33,** 996 (1987).

Levec, J., A. E. Saéz, and R. G. Carbonell, "The Hydrodynamics of Trickling Flow in Packed Beds: II. Experimental Observations," *AIChE J.*, **32,** 369 (1986).

Mata, A. R., and J. M. Smith, "Oxidation of Sulphur Dioxide in a Trickle-Bed Reactor," *Chem. Eng. J.*, **22,** 229 (1981).

Mills, P. L., and M. P. Duduković, "Evaluation of Liquid-Solid Contacting in Trickle-Bed Reactors by Tracer Methods," *AIChE J.*, **27,** 893, (1981); Erratum, **28,** 526 (1982).

Morita, S., and J. M. Smith, "Mass Transfer and Contacting Efficiency in a Trickle Bed Reactor," *Ind. Eng. Chem. Fund.*, **17,** 113 (1978).

Rao, V. G., and A. A. H. Drinkenburg, "Solid-Liquid Mass Transfer in Packed Beds with Cocurrent Gas-Liquid Downflow," *AIChE J.*, **31,** 1059 (1985).

Satterfield, C. N., "Trickle-Bed Reactors," *AIChE J.*, **21,** 209 (1975).

Satterfield, C. N., M. W. Elk, and G. S. Bliss, "Liquid-Solid Mass Transfer in Packed Beds with Downward Concurrent Gas-Liquid Flow," *AIChE J.*, 24, 709 (1978).

Specchia, V., G. Baldi, and A. Gianetto, "Solid-Liquid Mass Transfer in Concurrent Two-Phase Flow through Packed Beds," *Ind. Eng. Chem. Process Des. Dev.*, **17,** 362 (1978).

Talmor, E., "Two-Phase Downflow through Catalyst Beds. Part 1. Flow Maps," *AIChE J.*, **23,** 868 (1977a).

Manuscript received Aug. 23, 1989, and revision received June 8, 1990.